

COVER PAGE

Document downloaded by @DAEL

Fri Nov 27 01:52:11 2026
For personal use

When automatic English translation is provided, only the original document is authentic.
The EAA cannot be held responsible of any translation error

Bibliographical reference

Acoustic Radiation from Two Concentric Cylindrical Shells with Periodic Supports and a Viscoelastic Perforated Outer Coating, X. W. Yin, H. F. Cui and S.G. Shen, Acta Acustica **vol. 95** (Number 5), 2009, pp. 823-832

DOI
https://doi.org/10.3813/AAA.918213

Acta Acustica united with Acustica
Vol. 95 (2009) 823 – 832

DOI 10.3813/AAA.918213

Acoustic Radiation from Two Concentric Cylindrical Shells with Periodic Supports and a Viscoelastic Perforated Outer Coating

X. W. Yin
Wuxi Branch, Jiangsu Institute of Special Equipment Safety Supervision and Inspection, 197-1, Zhenghe Avenue, Huishan Economic Development Zone, Wuxi, Jiangsu Province, China, 214171. x.w.yin@163.com

H. F. Cui
Wuxi Institute of Technology, Wuxi, Jiangsu Province, China, 214121

S.G. Shen
China Ship Scientific Research Center, Wuxi, Jiangsu Province, China, 214082

Summary
A solution is developed for the acoustic radiation from two concentric cylindrical shells which are connected by a set of periodic annular plates, and the outer of which is coated with a viscoelastic perforated layer. All the perforations in the coating have an identical cavity configuration with variable (thickness-dependent) cross-sections. The classical theory of Kennard type and the linear acoustic field equation are employed to simulate the two shells and their entrained fluid, respectively. It is assumed that only membrane motions exist in the annular plates, based on which a two dimensional membrane theory is employed to derive their reactive forces. The viscoelastic perforated coating is divided into many sub-layers each has an equivalent complex wave number by using a thick walled cylinder model. Transfer matrix method is then used to develop the relation between the quantities (velocity and pressure) at the inner and outer surfaces of the coating. The solution is found by using Fourier wave number transforms, and the stationary phase approximation is used to find an expression for the far field pressure. Comparison of numerical results for the two concentric infinite cylindrical shells without the outer coating to measured data from a cabin model is in good agreement. Far field acoustic pressure results are presented for two cylindrical shells with and without the viscoelastic perforated coating, which indicate that the viscoelastic perforated coating can effectively reduce the radiated sound pressure at middle and high frequency ranges. The influences of the coating parameters on far field acoustic pressure are also discussed.

PACS no. 43.30.Jx

1. Introduction

Cylindrical shells are often found in various engineering applications ranging from large civil and mechanical structures to small electrical components. Due to their importance, constant attentions have been drawn on the acoustic and vibrational characteristics of the shells with internal structures [1, 2, 3, 4, 5, 6], fluid loadings [7, 8, 9] for more than half a century. In most of the publications, the dynamics of the internal structures (frames, rings or plates etc) and the entrained fluid are taken into account in the form of the reactive loadings at their interfaces, i.e., in impedance (stiffness) form [1, 2, 3, 4] or in receptance (mobility) form [5, 6]. Furthermore, the corresponding problems such as to what extent their dynamic characteristics affect the overall structures are so important that they received long-lasting and intensive investigations, and some well-known mechanisms such as wavenumber conversion [2, 3], vibration resonance [6] were found significantly altering the acoustic and vibrational characteristics of the combined structures.

Besides, in noise-control applications, the cylindrical shells are often coated with viscoelastic layers [10, 11, 12] into which perforations or inclusions are imbedded on certain occasions. Gaunaurd and his colleagues [13, 14] extended Kelvin–Voigt viscoelastic model to Navier's equation of elasticity for the coupling between viscoelastic coating and structures. Laulagnet and Guyader [10, 11] used the approximate solutions of Navier's equations to model the homogenous viscoelastic layer. Chen *et al.* [12] adopted Laulagnet's method for the problem of double cylindrical shell coated with homogenous viscoelastic layer. Nevertheless, when the coating contains perforations or inclusions, the above-mentioned homogenous

Received 19 July 2007,
accepted 20 April 2009.

© S. Hirzel Verlag · EAA

models can not be directly adopted since inhomogeneity may arise in the thickness direction or in other directions. Gilbert [15] proposed an updated Gilbert-Backus formula, i.e., in transfer matrix form, to obtain an exact solution for wave propagation in periodically stratified medium of arbitrary thickness. Song and Bolton [16] obtained the elements of the transfer matrix for a porous material through measurement.

Up to now, little attentions are drawn on the dynamics of cylindrical shells which are both connected with internals and coated with perforated coatings since any one of the above two subjects is quite complex and has not yet been adequately addressed. In the present paper, governing equations of two concentric cylindrical shells are developed, which includes the reactive loadings from the internal rings, the periodic annular plates, the entrained fluid and the perforated coating. Solutions to the far field acoustic radiation from the outer coating are obtained. Predicted results from two infinite cylindrical shells with periodic supports are compared to measured data taken on an immersed, point-driven two-walled cabin. The influences of coating parameters on acoustic radiation are also offered.

2. Theory

Two concentric infinite thin cylindrical shells, the outer of which is coated with a viscoelastic layer, are centered on the x-axis as shown in Figure 1. In the coating are symmetrically and uniformly arranged with vacuum perforations of one defined cavity shape which has variable cross sections with the change of thickness (see Figure 2a). The radius of the inner shell is given by a_1 and the thickness by h_1, while the radius of the outer shell is given by a_2 and the thickness by h_2. The interior of inner shell is *in vacuo*, the outer coating with total thickness of h_3 is surrounded by fluid, and fluid also exists in the annular space between the two shells. One set of periodically spaced rings are attached to the inner shell and another set of periodically spaced annular plates connect the inner and the outer shells. The inner shell is driven with a point force F_1 located at $r = a_1$, $x = x_0$, $\varphi = \varphi_0$ in cylindrical coordinates. The force is harmonic and has the time dependence of $\exp(-\mathrm{j}\omega t)$, where ω is angular frequency and t is the time. For algebraic convenience, $\exp(-\mathrm{j}\omega t)$ will henceforth be suppressed.

According to Figure 1, we consider that the rings, the fluid, the annular plates, and the coating exert reactive forces on the two shells. The loadings acting on the inner shell are the following: the point force, the fluid loading due to the interior fluid, the reactive loadings due to the rings as well as the annular plates, and the loadings on the outer shell are the fluid loading due to the interior fluid, the annular plates, and the loading due to the viscoelastic perforated coating, which may include the contribution from the fluid loading due to the exterior fluid.

The following assumptions are made in deriving the solutions that describe the vibration of and acoustic radiation from two concentric cylindrical shells.

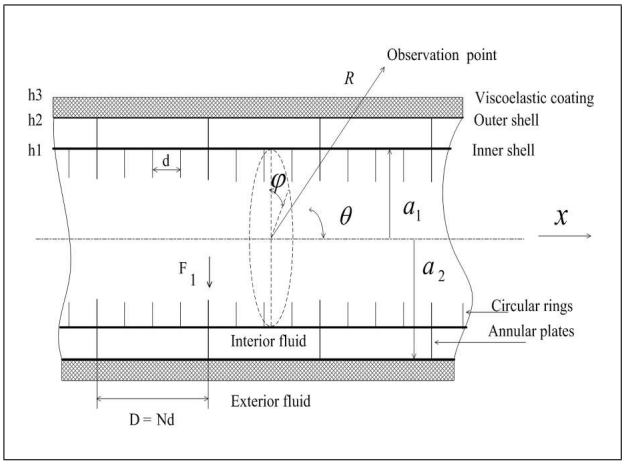

Figure 1. Two concentric cylindrical shells with doubly periodical stiffened members and viscoelasitc perforated outer coating.

1. All the loadings including the point force and the pressures acting on the shells and the coating are prescribed to be positive when they are directed outward from the center of the shells. The displacements of the shells and the surfaces of the coating are prescribed to be positive when they are directed outwards.
2. The ring supports interact with the inner shell only through normal forces along the circular lines of intersection with the inside surface of the shell. The ring supports do not apply moments or shear forces to the shell.
3. The annular plates interact with the two shells only through membrane forces along the circular lines of intersection with the inside surface of the shells. The annular plates do not apply moments or shear forces to the shell. Only membrane motions are taken into account in the plates.
4. The viscoelastic perforated coating is divided into many sub-layers each is perforated with a vacuum hole with a constant radius, and has an equivalent complex wave number to that of a homogenous sub-layer, i.e., without any perforations.
5. The observation point (R, θ, φ) for the acoustic radiation is located in the farfield, such as $k_0 R \gg 1$, where k_0 is the acoustic wave number and R is the radial distance of the observation point from the origin point.

2.1. Shell equations

In frequency ranges well below the critical frequency of the shell, Kennard thin shell theory is sufficiently accurate and may be adopted here for motions of the inner and the outer shells by application of the Fourier transforms into K-space [2]

$$\tilde{Z}^S_{1n}(k)\dot{\tilde{w}}_{1n}(k) = \tilde{f}_n - \tilde{p}_{1n} - \tilde{p}_{rn} - \tilde{p}_{b1n}, \quad (1)$$

$$\tilde{Z}^S_{2n}(k)\dot{\tilde{w}}_{2n}(k) = \tilde{p}_{2n} - \tilde{p}_{3n} + \tilde{p}_{b2n}, \quad (2)$$

where $\dot{\tilde{w}}_{1n}(k)$ and $\dot{\tilde{w}}_{2n}(k)$ are the transformed radial velocities of the inner and outer shells, respectively, and $\tilde{Z}^S_{1n}(k)$ and $\tilde{Z}^S_{2n}(k)$ (see Appendix A1) are the transformed

impedances of the inner and outer shells at the n-th circumferential mode, respectively. $\tilde{f}_n$, $\tilde{p}_{1n}$, $\tilde{p}_{rn}$, $\tilde{p}_{b1n}$, are the loadings on the inner shell at the n-th circumferential mode in K-space due to the point force, the interior fluid, the rings and the annular plates, respectively. $\tilde{f}_{2n}$, $\tilde{p}_{3n}$, $\tilde{p}_{b2n}$, are the loadings on the outer shell at the n-th circumferential mode in K-space due to the interior fluid, the viscoelastic coating and the annular plates, respectively. The loadings due to the periodical rings and the point force were given by Burroughs [2, 3], which are expressed in Appendix A2. The loadings due to the annular plates and the viscoelastic perforated coating are derived in sections 2.3 and 2.4, respectively.

2.2. Fluid field equation and its solution

Yeh and Chen [9] studied the coupling between a double cylindrical shell and the entrained viscous fluid. However, the problems such as to what extent the viscosity of fluid influences the vibration and sound radiation from the shell structures were not adequately addressed. In the present paper, Yoshikawa's conventional method [8] for double shell is adopted, assuming that the fluid is inviscid, irrotational, and compressible.

The pressure in the acoustic medium satisfies the following reduced wave equation in cylindrical coordinates ($i = 1, 2$ for interior fluid; $i = 4$ for exterior fluid)

$$\nabla_r^2 p_i(x, r, \varphi) + k_0^2 p_i(x, r, \varphi) = 0. \tag{3}$$

Taking the Fourier transform with respect to the x-axis,

$$\left(\frac{1}{r^2}\frac{\partial^2}{\partial\varphi^2} + \frac{1}{r}\frac{\partial}{\partial r}\left(r\frac{\partial}{\partial r}\right) + \left(k_0^2 - k^2\right)\right)\tilde{p}_i = 0. \tag{4}$$

The solution of equation (4) can be determined by making use of the radiation conditions at and the boundary conditions at interfaces between the fluid and the shells as well as the coating. So the loadings on the two shells due to the fluid in equations (1)–(2) can be given in the following forms,

$$\tilde{p}_{1n} = G_{f12}(k, a_1)\dot{\tilde{w}}_{1n} + G_{f21}(k, a_1)\dot{\tilde{w}}_{2n}, \tag{5}$$

$$\tilde{p}_{2n} = G_{f12}(k, a_2)\dot{\tilde{w}}_{1n} + G_{f21}(k, a_2)\dot{\tilde{w}}_{2n}, \tag{6}$$

$$\tilde{p}_{4n} = G_{f3}(k, a_3)\dot{\tilde{w}}_{3n}, \tag{7}$$

where $a_3 = a_2 + h_3$ is the radius of the outer surface of the viscoelastic coating, and $\dot{\tilde{w}}_{3n}$ is the transformed radial velocity of the outer surface of the coating at the n-th circumferential shell mode. And the quantities G_{f12}, G_{f21}, G_{f3} are defined as

$$G_{f12}(k, r) = \tag{8a}$$

$$\begin{cases} \frac{\mathrm{i}\rho\omega}{\sqrt{k_0^2-k^2}}\Big[J_n\big(\sqrt{k_0^2-k^2}r\big)N_n'\big(\sqrt{k_0^2-k^2}a_2\big) \\ \qquad -J_n'\big(\sqrt{k_0^2-k^2}a_2\big)N_n\big(\sqrt{k_0^2-k^2}r\big)\Big] \\ \qquad \cdot\Big[J_n'\big(\sqrt{k_0^2-k^2}a_1\big)N_n'\big(\sqrt{k_0^2-k^2}a_2\big) \\ \qquad -J_n'\big(\sqrt{k_0^2-k^2}a_2\big)N_n'\big(\sqrt{k_0^2-k^2}a_1\big)\Big]^{-1} \\ \qquad\qquad (k_0 > k), \\ \frac{\mathrm{i}\rho\omega}{\sqrt{k^2-k_0^2}}\Big[I_n\big(\sqrt{k^2-k_0^2}r\big)K_n'\big(\sqrt{k^2-k_0^2}a_2\big) \\ \qquad -I_n'\big(\sqrt{k^2-k_0^2}a_2\big)K_n\big(\sqrt{k^2-k_0^2}r\big)\Big] \\ \qquad \cdot\Big[I_n'\big(\sqrt{k^2-k_0^2}a_1\big)K_n'\big(\sqrt{k^2-k_0^2}a_2\big) \\ \qquad -I_n'\big(\sqrt{k^2-k_0^2}a_2\big)K_n'\big(\sqrt{k^2-k_0^2}a_1\big)\Big]^{-1} \\ \qquad\qquad (k_0 < k), \end{cases}$$

$$G_{f21}(k, r) = \tag{8b}$$

$$\begin{cases} \frac{\mathrm{i}\rho\omega}{\sqrt{k_0^2-k^2}}\Big[J_n\big(\sqrt{k_0^2-k^2}r\big)N_n'\big(\sqrt{k_0^2-k^2}a_1\big) \\ \qquad -J_n'\big(\sqrt{k_0^2-k^2}a_1\big)N_n\big(\sqrt{k_0^2-k^2}r\big)\Big] \\ \qquad \cdot\Big[J_n'\big(\sqrt{k_0^2-k^2}a_1\big)N_n\big(\sqrt{k_0^2-k^2}a_2\big) \\ \qquad -J_n'\big(\sqrt{k_0^2-k^2}a_2\big)N_n'\big(\sqrt{k_0^2-k^2}a_1\big)\Big]^{-1} \\ \qquad\qquad (k_0 > k), \\ \frac{\mathrm{i}\rho\omega}{\sqrt{k^2-k_0^2}}\Big[I_n\big(\sqrt{k^2-k_0^2}r\big)K_n'\big(\sqrt{k^2-k_0^2}a_1\big) \\ \qquad -I_n'\big(\sqrt{k^2-k_0^2}a_1\big)K_n\big(\sqrt{k^2-k_0^2}r\big)\Big] \\ \qquad \cdot\Big[I_n'\big(\sqrt{k^2-k_0^2}a_1\big)K_n\big(\sqrt{k^2-k_0^2}a_2\big) \\ \qquad -I_n'\big(\sqrt{k^2-k_0^2}a_2\big)K_n'\big(\sqrt{k^2-k_0^2}a_1\big)\Big]^{-1} \\ \qquad\qquad (k_0 < k), \end{cases}$$

$$G_{f3}(k, r) = \begin{cases} \frac{\mathrm{i}\rho\omega}{\sqrt{k_0^2-k^2}}\frac{H_n^{(1)}\big(\sqrt{k_0^2-k^2}r\big)}{H_n^{(1)\prime}\big(\sqrt{k_0^2-k^2}a_3\big)} & (k_0 > k), \\ \frac{\mathrm{i}\rho\omega}{\sqrt{k_0^2-k^2}}\frac{K_n\big(\sqrt{k_0^2-k^2}r\big)}{K_n'\big(\sqrt{k_0^2-k^2}a_3\big)} & (k_0 > k). \end{cases} \tag{8c}$$

From equations (5)–(6), the pressure on the inner shell includes two parts: one is induced by the vibration of the inner shell with the impedance of $G_{f12}(k, a_1)$, the other by the vibration of the outer shell with the impedance of $G_{f21}(k, a_1)$. Similarly, the pressure on the outer shell contains two parts: one is induced by the vibration of the inner shell with the impedance of $G_{f12}(k, a_1)$, the other by the vibration of the outer shell with the impedance of $G_{f21}(k, a_1)$. The coefficients $G_{f21}(k, r)$ and $G_{f12}(k, r)$ reveal the fluid-shell coupling effect, i.e., a feedback loop, which controls the coupled vibrations the double shell. However, for exterior field, i.e., the pressure on the outer surface of the coating is only attributed to its surface vibration.

According to Junger and Feit [17] and with inspection of equations (8a)–(8c), further information would be readily obtained as

1. $G_{f12}(k,r)$, $G_{f21}(k,r)$ and $G_{f3}(k,r)$ are complex, the real parts of which are resistive impedances corresponding to the radiation damping while the imaginary parts are reactive impedances corresponding to the attached mass.
2. For the interior fluid, with $k_0 > k$ or not, $G_{f12}(k,r)$ and $G_{f21}(k,r)$ are purely imaginary, which means that the interior fluid will supply attached mass for the shells. However, it is not the case for the exterior fluid. When $k_0 > k$, $G_{f3}(k,r)$ has both real and imaginary parts, and when $k_0 < k$, $G_{f3}(k,r)$ is purely imaginary.

2.3. Reactive forces by periodically spaced annular plates

When two cylindrical shells are connected by a set of annular plates, forces and moments are coupled at their attachments. Klauson and Metsaveer [4], Cuschieri [5], Guo [6] have investigated a cylindrical shell with internal plate(s), the forces and moments at the junctions of the shell and the plate(s) are taken into account by using receptance (or mobility) approach. For simplification, in this section, only membrane motions in annular plates are in consideration, thus the coupling moments at their attachment will be omitted. Its validation will be made through comparisons between numerical results and measured data from a cabin model in section 3.1. In two dimensional cylindrical coordinates, membrane motions in an annular plate [18] are employed as follows

$$\nabla_r^2 w_b(r,\varphi) + k_b^2 w_b(r,\varphi) = 0, \tag{9}$$

where $w_b(r,\varphi)$ is the radial displacement for the annular plate. k_b is the radial wave number for quasi-longitudinal waves in the plates. Equation (9) is a well known Bessel equation in cylindrical coordinates, which has the general solution

$$w_b(r,\varphi) = \sum_{-\infty}^{+\infty} \Big(A_{bn} J_n(k_b r) + B_{bn} N_n(k_b t) \Big) \cdot \exp\big(\mathrm{j}n\varphi\big). \tag{10}$$

When enforcing the compatibility of radial displacements between the shells and the plates at their junctions ($x = qD$, $q = -\infty, +\infty$), its coefficients A_{bn} and B_{bn} can be determined in terms of the velocities of the inner shell and outer shell as

$$A_{bn} = \frac{1}{-\mathrm{j}\omega} \frac{\dot{w}_{1n}(qD) N_n(k_b a_2) - \dot{w}_{2n}(qD) N_n(k_b a_1)}{J_n(k_b a_1) N_n(k_b a_2) - J_n(k_b a_2) N_n(k_b a_1)}, \tag{11}$$

$$B_{bn} = \frac{1}{-\mathrm{j}\omega} \frac{-\dot{w}_{1n}(qD) N_n(k_b a_2) + \dot{w}_{2n}(qD) N_n(k_b a_1)}{J_n(k_b a_1) N_n(k_b a_2) - J_n(k_b a_2) N_n(k_b a_1)}. \tag{12}$$

Substituting equations (11)–(12) into equation (10) and separating it into two terms with the coefficients

$$Z_{b1} = \frac{1}{-\mathrm{j}\omega} \frac{J_n(k_b r) N_n(k_b a_2) - N_n(k_b r) J_n(k_b a_2)}{J_n(k_b a_1) N_n(k_b a_2) - J_n(k_b a_2) N_n(k_b a_1)}, \tag{13}$$

$$Z_{b2} = \frac{1}{-\mathrm{j}\omega} \frac{-J_n(k_b r) N_n(k_b a_1) + N_n(k_b r) J_n(k_b a_1)}{J_n(k_b a_1) N_n(k_b a_2) - J_n(k_b a_2) N_n(k_b a_1)}. \tag{14}$$

Equations (13)–(14) are the expressions of radial displacement impedances by annular plates at the n-th circumferential mode. Radial displacement of the plates can be written as

$$w_b(r,\varphi) = \sum_{-\infty}^{+\infty} \Big(Z_{b1} \dot{w}_{1n}(qD) + Z_{b2} \dot{w}_{2n}(qD) \Big) \cdot \exp\big(\mathrm{j}n\varphi\big). \tag{15}$$

Equation (15) should satisfy the boundary conditions

$$p_{b1}(a_1,\varphi) = \sum_{-\infty}^{+\infty} \delta(x - qD) Et \frac{\partial w_b(r,\varphi)}{\partial r}\Big|_{r=a_1},$$

$$p_{b2}(a_2,\varphi) = -\sum_{-\infty}^{+\infty} \delta(x - qD) Et \frac{\partial w_b(r,\varphi)}{\partial r}\Big|_{r=a_2}. \tag{16}$$

In K-space, the applied forces at the n-th circumferential mode due to the annular plates are

$$\begin{aligned} \tilde{p}_{b1} &= \frac{Eh}{2\pi} \sum_{-\infty}^{+\infty} \sum_{-\infty}^{+\infty} \exp\big(-\mathrm{j}kqD\big) \\ &\quad \cdot \Big[\frac{\partial Z_{b1}(a_1,k_b)}{\partial r} \dot{w}_{1n}(qD) + \frac{\partial Z_{b2}(a_1,k_b)}{\partial r} \dot{w}_{2n}(qD) \Big] \\ &\quad \cdot \exp\big(\mathrm{j}n\varphi\big) \\ \tilde{p}_{b2} &= -\frac{Eh}{2\pi} \sum_{-\infty}^{+\infty} \sum_{-\infty}^{+\infty} \exp\big(-\mathrm{j}kqD\big) \\ &\quad \cdot \Big[\frac{\partial Z_{b1}(a_2,k_b)}{\partial r} \dot{w}_{1n}(qD) + \frac{\partial Z_{b2}(a_2,k_b)}{\partial r} \dot{w}_{2n}(qD) \Big] \\ &\quad \cdot \exp\big(\mathrm{j}n\varphi\big), \end{aligned} \tag{17}$$

where

$$\dot{w}_{1n}(qD) = \int_{-\infty}^{+\infty} \dot{\tilde{w}}_{1n}(k') \exp\big(\mathrm{j}k'qD\big)\,\mathrm{d}k', \tag{18}$$

$$\sum_{q=-\infty}^{+\infty} \dot{w}_{1n}(qD) \exp\big(-\mathrm{j}kqD\big) = \sum_{q=-\infty}^{+\infty} \int_{-\infty}^{+\infty} \dot{\tilde{w}}_{1n}(k') \exp\big(-\mathrm{j}(k-k')qD\big)\,\mathrm{d}k'. \tag{19}$$

Using Poisson summation formula then yields

$$\begin{aligned} &\sum_{q=-\infty}^{+\infty} \dot{w}_{1n}(qD) \exp\big(-\mathrm{j}kqD\big) \\ &\quad = 2\pi \sum_{q=-\infty}^{+\infty} \int_{-\infty}^{+\infty} \dot{\tilde{w}}_{1n}(k') \delta\big((k'-k)D - 2q\pi\big)\,\mathrm{d}k' \\ &\quad = k_D \sum_{q=-\infty}^{+\infty} \dot{\tilde{w}}_{1n}(k + qk_D), \end{aligned} \tag{20}$$

where $k_D = 2\pi/D$, h is the thickness of the plates. According to equation (20), the n-th mode component of

equation (17) can be expressed as

$$\tilde{p}_{b1n} = \frac{k_D E h}{2\pi} \sum_{q=-\infty}^{+\infty} \Big[\frac{\partial Z_{b1}(a_1, k_b)}{\partial r} \dot{\tilde{w}}_{1n}(k + qk_D) + \frac{\partial Z_{b2}(a_1, k_b)}{\partial r} \dot{\tilde{w}}_{2n}(k + qk_D) \Big],$$

$$\tilde{p}_{b2n} = -\frac{k_D E h}{2\pi} \sum_{q=-\infty}^{+\infty} \Big[\frac{\partial Z_{b1}(a_2, k_b)}{\partial r} \dot{\tilde{w}}_{1n}(k + qk_D) + \frac{\partial Z_{b2}(a_2, k_b)}{\partial r} \dot{\tilde{w}}_{2n}(k + qk_D) \Big]. \quad (21)$$

Rewriting equation (21) in a concise form,

$$\tilde{p}_{b1n} = \frac{k_D E h}{2\pi} \sum_{q=-\infty}^{+\infty} \Big[G_{b11}(a_1) \dot{\tilde{w}}_{1n}(k + qk_D) + G_{b12}(a_1) \dot{\tilde{w}}_{2n}(k + qk_D) \Big],$$

$$\tilde{p}_{b2n} = -\frac{k_D E h}{2\pi} \sum_{q=-\infty}^{+\infty} \Big[G_{b21}(a_2) \dot{\tilde{w}}_{1n}(k + qk_D) + G_{b22}(a_2) \dot{\tilde{w}}_{2n}(k + qk_D) \Big], \quad (22)$$

From equation (22), it is clearly found that the presence of periodically spaced members, i.e., plates, may transform elastic waves with wave number of k to infinite partial waves with a wave number shift which is uniquely determined by the stiffening members' interval.

2.4. Reactive forces by the viscoelastic perforated coating

The cavity configuration of the viscoelastic perforated coating is illustrated in Figure 2a and the perforations are symmetric and periodic with the axis of one arbitrary hole. The radius of the perforation varies with the thickness of the coating.

Song and Bolton [16] have modeled the perforated materials as fluids having complex properties which they measured in a conventional, two-microphone standing wave tube with transfer matrix method. Yin [19] also modeled the viscoelastic perforated coating as fluids with equivalent complex moduli by regarding it as a stratified coating with multiple homogenous viscoelasitc sub-layers.

In Figure 2a, we divide the coating into many prescribed sub-layers each has uniform perforations. For the i-th sub-layer, the transfer matrix is written as [16]

$$[T_i] = \begin{bmatrix} \cos(k_{a,i}\Delta l_i) & i\rho_{a,i}c_{a,i}\sin(k_{a,i}\Delta l_i) \\ i\sin(k_{a,i}\Delta l_i)/\rho_{a,i}c_{a,i} & \cos(k_{a,i}\Delta l_i) \end{bmatrix}, \quad (23)$$

where $\rho_{a,i}$, $c_{a,i}$, $k_{a,i}$ are the density, phase velocity, wave number for the i-th sub-layer and Δl_i is the thickness of the i-th sub-layer. When the sub-layer is homogenous, i.e., it has no inclusions or perforations, at any prescribed specific frequency and temperature, $c_{a,i}$ is only dependent on its material properties. However, in case that perforations are embedded, inhomogeneity may arise, so elastic waves may reflect and refract at the interfaces of the perforations, i.e., $c_{a,i}$ and $k_{a,i}$ would be different for different perforated sub-layers.

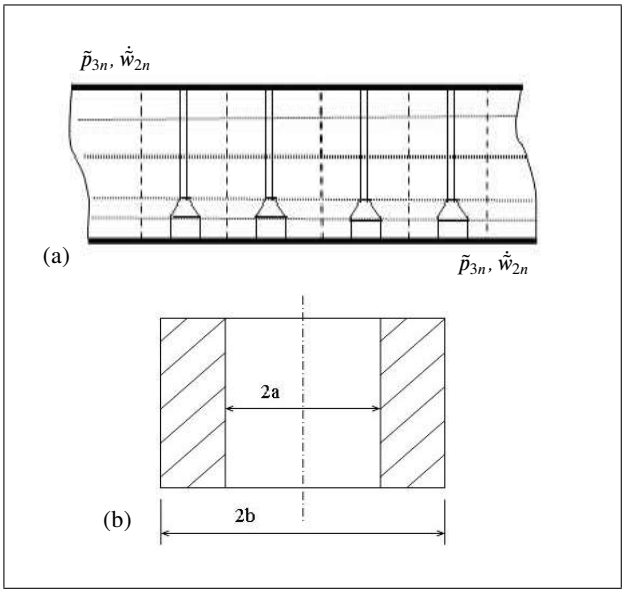

Figure 2. Schematic illustration of viscoelastic perforated coating. (a) The interior configuration of the perforated coating. (b) Cylinder model.

According to the above-mentioned features of the coating, one cylinder with two radii of a and b is picked out from one sub-layer, which is depicted in Figure 2b. Under symmetric boundary conditions, Lamé's equation of elasticity in the cylindrical coordinate system is applied to the cylinder, and the equivalent complex wave number for the sub-layer with porosity ratio of $\varepsilon = a/b$ is obtained as [19]

$$\overline{k}_{a,i} = k_l^2 \Big(1 + \frac{\lambda}{\mu(1 - \mathrm{i}\eta)} \frac{\varepsilon^2}{1 - \varepsilon^2} \Big), \quad (24)$$

where k_l, λ and μ are the longitudinal wave number and two Lamé constants of homogenous viscoelastic materials, respectively, η is the loss factor.

The longitudinal wave number of homogenous viscoelastic materials is frequency dependent, i.e., $k_l^2 = \rho_{a,i}\omega^2/(\lambda + 2\mu)$. So from equation (24), is the equivalent complex wave number that may transform the dynamic problem of perforated sub-layer to that of a homogenous sub-layer. Also from equation (24), the term including the porosity ratio is quadratic, while the two Lamé constants are linear, so we can simply deduce that the equivalent complex wave number would be more sensitive to the change of the porosity radio.

From equation (23), pressures and normal velocities of the two surfaces of the viscoelastic perforated coating satisfy the relation

$$\begin{Bmatrix} \tilde{p}_{4n} \\ \dot{\tilde{w}}_{3n} \end{Bmatrix} = \begin{bmatrix} a_{11} & a_{12} \\ a_{21} & a_{22} \end{bmatrix} \begin{Bmatrix} \tilde{p}_{3n} \\ \dot{\tilde{w}}_{2n} \end{Bmatrix}, \quad (25)$$

where a_{ij} $(i = 1, 2;\ j = 1, 2)$ are the transfer functions for viscoelastic perforated coating, which are obtained from

the following matrix multiplication, i.e., $[T_1][T_2]\ldots[T_n]$ (n is the number of the sub-layer). With combination of equation (25) and equation (7), we can obtain

$$\dot{\tilde{w}}_{3n} = \frac{a_{11}a_{22} - a_{12}a_{21}}{a_{11} - a_{21}G_{f3}(k, a_3)}\dot{\tilde{w}}_{2n}, \tag{26}$$

$$\tilde{p}_{3n} = \frac{G_{f3}(k, a_3)a_{22} - a_{12}}{a_{11} - a_{21}G_{f3}(k, a_3)}\dot{\tilde{w}}_{2n}. \tag{27}$$

If we define the expressions

$$\beta_1 = \frac{a_{11}a_{22} - a_{12}a_{21}}{a_{11} - a_{21}G_{f3}(k, a_3)},$$

$$\beta_1 = \frac{G_{f3}(k, a_3)a_{22} - a_{12}}{a_{11} - a_{21}G_{f3}(k, a_3)}, \tag{28}$$

the relations between the quantities (velocities, pressures) of the upper and lower surfaces of the viscoelastic coating are written in the following concise form

$$\dot{\tilde{w}}_{3n} = \beta_1\dot{\tilde{w}}_{2n}, \tag{29}$$

$$\tilde{p}_{3n} = \beta_2\dot{\tilde{w}}_{2n}. \tag{30}$$

Equation (30) expresses the reactive loading on the outer shell due to the viscoelastic perforated coating, which involves the contribution from the exterior fluid.

2.5. Solution for acoustic radiation

By substituting equations (5)–(6), equation (22) and equation (30) into equations (1)–(2), and using Burrough's formula [2, 3] for point force and reactive forces by rings, the following governing equations are obtained,

$$\begin{aligned}\tilde{Z}^S_{1n}\dot{\tilde{w}}_{1n} &= F_n - G_{f12}(a_1)\dot{\tilde{w}}_{1n} - G_{f21}(a_1)\dot{\tilde{w}}_{2n} \\ &\quad - Z^r_n S_d\{\dot{\tilde{w}}_{1n}\} + G_{b11}(a_1)S_D\{\dot{\tilde{w}}_{1n}\} \\ &\quad + G_{b12}(a_1)S_D\{\dot{\tilde{w}}_{2n}\}, \\ \tilde{Z}^S_{2n}\dot{\tilde{w}}_{2n} &= G_{f12}(a_1)\dot{\tilde{w}}_{1n} + G_{f21}(a_2)\dot{\tilde{w}}_{2n} \\ &\quad - G_{b21}(a_2)S_D\{\dot{\tilde{w}}_{1n}\} \\ &\quad - G_{b22}(a_2)S_D\{\dot{\tilde{w}}_{2n}\} - \beta_2\dot{\tilde{w}}_{2n},\end{aligned} \tag{31}$$

where the operators $S_d\{\ \}$, $S_D\{\ \}$ [2] are often used for periodically spaced structures and have the forms

$$S_d\{A(k)\} = \frac{k_d}{2\pi}\sum_{m=-\infty}^{\infty} A(k + mk_d),$$

$$S_D\{A(k)\} = \frac{k_D}{2\pi}\sum_{m=-\infty}^{\infty} A(k + mk_D). \tag{32}$$

Inspection of equation (31) shows that the vibration responses of the inner and outer shell are attributed to five parts: point force (F_n), the interior fluid ($-G_{f12}(a_1)\dot{\tilde{w}}_{1n} - G_{f21}(a_1)\dot{\tilde{w}}_{2n}, G_{f12}(a_2)\dot{\tilde{w}}_{1n} + G_{f21}(a_2)\dot{\tilde{w}}_{2n}$), the viscoelastic coating ($\beta_2\dot{\tilde{w}}_{2n}$), the rings ($-Z^r_n S_d\{\dot{\tilde{w}}_{1n}\}$), and the annular plates ($G_{b11}(a_1)S_D\{\dot{\tilde{w}}_{1n}\} + G_{b12}(a_1)S_D\{\dot{\tilde{w}}_{2n}\}$, $-G_{b21}(a_2)S_D\{\dot{\tilde{w}}_{1n}\} - G_{b22}(a_2)S_D\{\dot{\tilde{w}}_{2n}\}$). From equation (31), the two shells are coupled through the interior fluid,

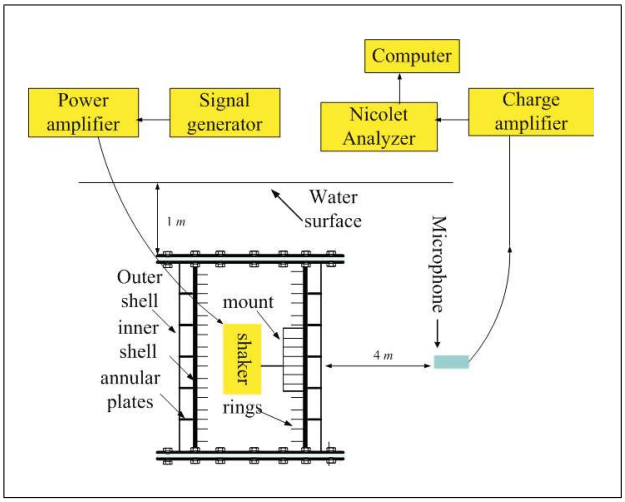

Figure 3. Sketch of the experimental setup for the underwater cabin model.

the annular plates, the coating and the exterior fluid simultaneously.

With very complicated derivation procedure, the radial velocity for the outer shell $\dot{\tilde{w}}_{2n}(k)$ can be solved. Thus, sound radiation pressure due to the outer shell can be expressed as ($k_0 > k$)

$$\tilde{p}_3(r, k, \varphi) = \tag{33}$$
$$\mathrm{j}\rho_0\omega\sum_{n=-\infty}^{\infty}\frac{\dot{\tilde{w}}_{3n}(k)H_n^{(1)}(\sqrt{k_0^2 - k^2}r)\exp(\mathrm{j}n\varphi)}{\sqrt{k_0^2 - k^2}H_n^{(1)'}(\sqrt{k_0^2 - k^2}a_3)}.$$

In farfield, asymptotic of equation (33) is as follows

$$\begin{aligned}\tilde{p}_3(r, k, \varphi) &= \mathrm{j}\rho_0\omega\sqrt{\frac{2}{\pi\sqrt{(k_0^2 - k^2)^3}r}} \\ &\quad\cdot\exp\left(\mathrm{j}\sqrt{k_0^2 - k^2}r - \pi/4\right) \\ &\quad\cdot\sum_{n=-\infty}^{\infty}\frac{\dot{\tilde{w}}_{3n}(k)\exp(\mathrm{j}n\varphi)(-\mathrm{j})^n}{H_n^{(1)'}(\sqrt{k_0^2 - k^2}a_3)}.\end{aligned} \tag{34}$$

Use of stationary phase method in taking the inverse Fourier transform of equation (34), the magnitude of the acoustic radiation pressure from the outer surface of the coating surrounding the double cylindrical shell is obtained as

$$|p_f| = \left|\frac{2\rho_0 c_0}{R\sin\theta}\sum_{n=-\infty}^{\infty}\frac{\beta_1(k_0\cos\theta)\,\dot{\tilde{w}}_{2n}(k_0\cos\theta)}{H_n^{(1)'}(k_0 a_3\sin\theta)}\cdot\exp(\mathrm{j}n\varphi)(-\mathrm{j})^n\right|. \tag{35}$$

3. Numerical calculation and discussion

3.1. Comparisons to experimental measurements

A two-walled cylindrical steel cabin is constructed. The inner shell is reinforced by one set of periodically spaced

Table I. Parameters of the cabin model.

Inner shell		**steel**	**Outer shell**		**steel**
density	ρ(Kg/m^3)	7.80×10^3	Poisson's ratio	ν	0.3
Young's modulus	E(N/m)	2.01×10^{11}	loss factor	η	0.002
mean radius	a_1(m)	0.5	mean radius	a_2(m)	0.585
thickness	h_1(m)	0.005	thickness	h_2(m)	0.005
length	l(m)	1.5	length	l(m)	1.5
Annular plates		**steel**	**Ending caps**		**steel**
thickness	t(m)	0.005	thickness	(m)	0.03
spacing	D(m)	0.3	**Fluid**		**water**
Rings		**steel**	density	ρ_0(Kg/m^3)	1.0×10^3
spacing	d(m)	0.10	sound velocity	c_0 (m/s)	1500
height	h_r(m)	0.045	**Driver**	**force**	1.0
thickness	t(m)	0.002	position	x_0, φ_0	0.0,0.0

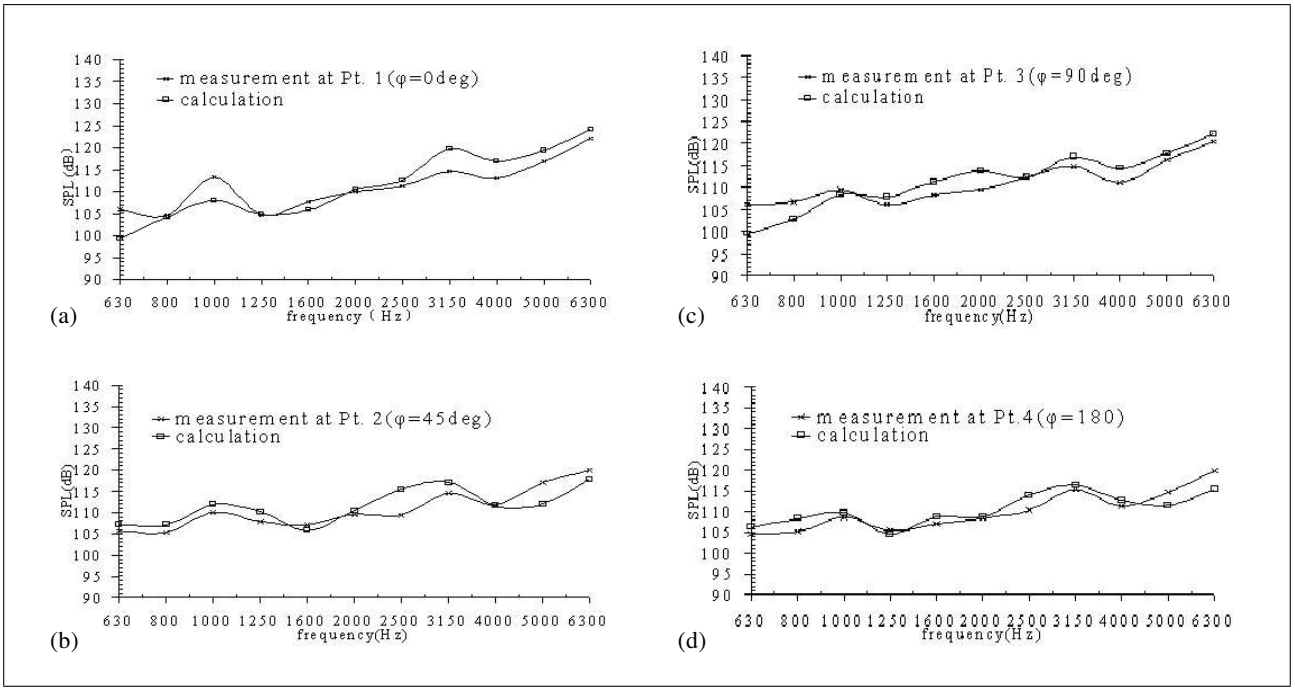

Figure 4. Comparison of numerical results for two infinite cylindrical shells to measured data from cabin model.
(a) $\varphi = 0°$, (b) $\varphi = 45°$, (c) $\varphi = 90°$, (d) $\varphi = 180°$.

rings, and the two shells are connected with another set of periodically spaced annular plates. Two ends of the cabin are closed using thick end caps. The parameters of the cabin are given in Table I and the setup of the measurement is illustrated in Figure 3. The cabin is immersed one meter below the water surface by using a ballast mass, and one hydrophone is placed in a fixed point four meters away from the nearest generate line of the cabin, then the observation points can be located through rotating the cabin.

Prior to making measurement of acoustic radiation from the cabin, the background noise was measured and guaranteed to have little impact on the acoustic radiation measurement. The cabin is driven by 1 N harmonic point force, and the sound pressures are measured at four observation points. Acoustic pressure levels with reference to 1 µPa and corrected to a distance of 1 m are presented. In Figure 4, numerical results for two infinite reinforced cylindrical shells are compared to measured data taken on a point-driven cabin model in water in 1/3 octave band. The difference between the predicted and the measured levels is within 5 dB above 630 Hz.

In most of the related publications [2, 19], experimental data from a finite cylindrical cabin is used to verify the numerical results for the infinite cylindrical shell, however, the applicability of finite cylindrical cabin need detailed discussion, e.g., the problems such as to what extent the length of the shells affects their structural and acoustic responses should be adequately addressed. According

Table II. Parameters of the viscoelastic materials.

Frequency (Hz)	λ (Mpa)	μ (Mpa)	η
100	200	5.80	0.36
125	200	5.80	0.36
163	200	5.80	0.36
200	200	5.80	0.36
250	200	5.80	0.36
315	200	5.80	0.36
400	200	5.80	0.36
500	200	5.80	0.36
630	200	5.80	0.36
800	200	5.80	0.36
1000	300	5.80	0.36
1250	300	4.80	0.36
1600	400	3.90	0.38
2000	600	4.156	0.415
2500	910	4.65	0.46
3150	1500	5.15	0.5
4000	2030	5.60	0.538

to basic concepts of vibration theory, i.e., mode superposition method, above the first resonance frequency when the cabin vibrates in beam type between two thick walled caps, the numerical results for the theoretical model of infinite cylindrical shell are acceptable. In our work, the frequency 630 Hz is far greater than the first natural frequency of bending as beam-type mode, and the predicted and measured results agree well. Nevertheless, more factors such as the testing basin's depth and radius, free surface and bottom conditions also have considerable influences on the measured data, which have not yet been adequately addressed in publications. The related works are strongly anticipated

3.2. Discussions on numerical results

The outer cylindrical shell is coated with viscoelastic perforated layer which has material properties with frequency dependence, namely, Lamé constans λ, μ and loss factor η. In this subsection, we will discuss the influences of the viscoelastic perforated coating and its material properties on sound radiation from two cylindrical shells with doubly periodic supports.

3.2.1. Acoustic radiation comparison between the bare shells and the coated shells

Material properties of the viscoelastic coating made of general rubber have been measured at 20 °C within frequency range of 4000 Hz and its main parameters are listed in Table II. The coating has total thickness of 70 mm and density of 1143 kg/m^3. Its porosity ratio ε varies from 0.12 to 0.66 at different sub-layer. Numerical results for the acoustic radiation from two cylindrical shells with doubly periodic supports and the viscoelastic perforated coating are presented in Figure 5.

From Figure 5, the numerical results indicate that below 400 Hz, viscoelastic perforated coating has weak influence on the acoustic radiation, while above 400 Hz, it can effectively reduce the acoustic radiation from the outer shell.

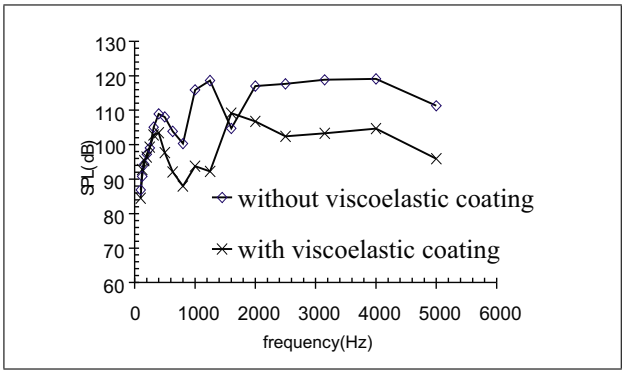

Figure 5. Comparison of numerical results for cylindrical shells with and without viscoelastic perforated coating.

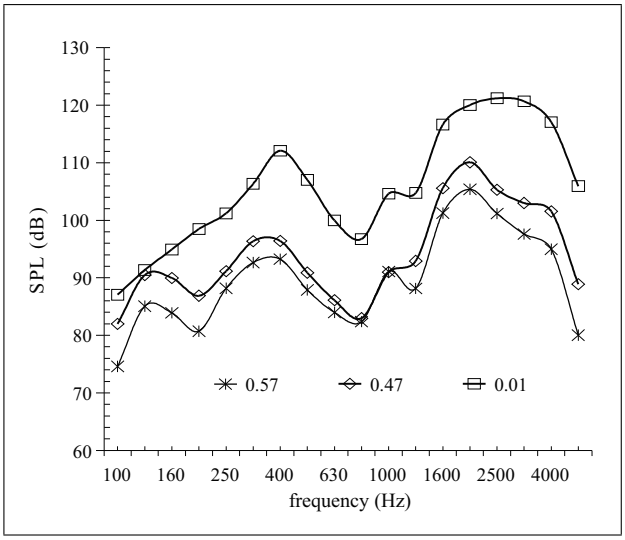

Figure 6. Influence of coating with different porosity ratios on radiated pressure.

The acoustic attenuation effects of viscoelastic or damping materials are well known, however, the influences of the viscoelastic material parameters and porosity ratios have not yet been fully addressed, which will be discussed in next subsection.

3.2.2. Influences of parameters of the coating on the acoustic radiation

To further reveal how the coating influences the acoustic radiation from two cylindrical shells with periodic supports, we alter the coating parameters (porosity ratios, Lamé constants, loss factors) to calculate the far field acoustic pressure. From Figure 6, porosity ratio can strongly influence the acoustic pressure which will decreases with the increase of the porosity ratio. According to theoretical acoustics, compared to compressive waves, shear waves are more liable to dissipate vibrating or sound energy during their propagation in some viscoelastic materials, such as rubber, plastic. To some extent, the increase of porosity ratio means the coating has more capacity of transforming compressive waves into shear waves.

From Figure 7 and Figure 8, the loss factor η and the bulk modulus λ have little impact on the acoustic radiation.

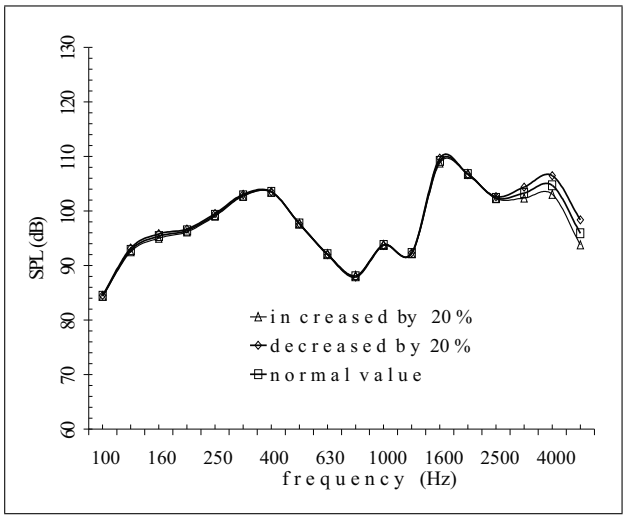

Figure 7. Influence of coating with different loss factors on radiated pressure.

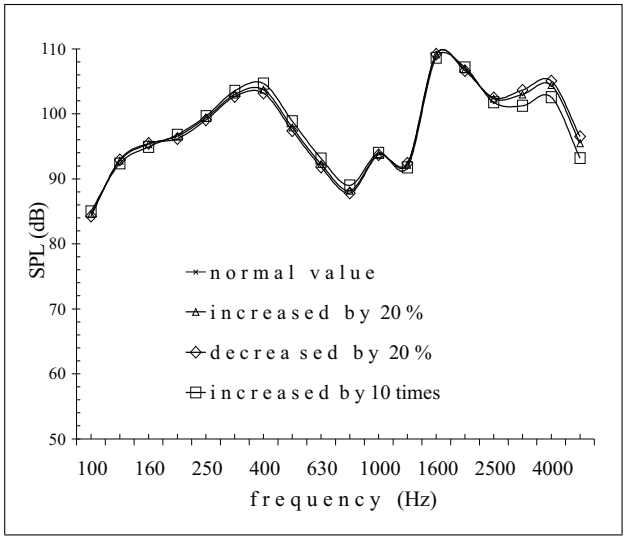

Figure 8. Influence of coating with different bulk modulus λ on radiated pressure.

In the present paper, the main mechanism of the acoustic attenuation comes from the wave transforms and the energy dissipation of shear waves according to the theoretical model, which indicates that the bulk modulus and loss factor play a minor role in acoustic radiation. In case that the coating is homogenous, and as reported by Laulagnet and Guyader [11], Chen and her colleagues [12], the elastic modulus and loss factor have fairly effects on the acoustic radiation.

From Figure 9, the acoustic pressure decreases 1 dB almost in all calculation frequency ranges when shear modulus μ is increased by 20 percent. Moreover, when the shear modulus is increased by 10 times, the radiation pressure will decrease by 5–10 dB above 400 Hz. In contrast to bulk modulus λ, shear modulus μ plays an apparently important role in sound attenuation.

So from Figures 6–9, porosity ratio and shear modulus are the dominant factors for noise control, which will be

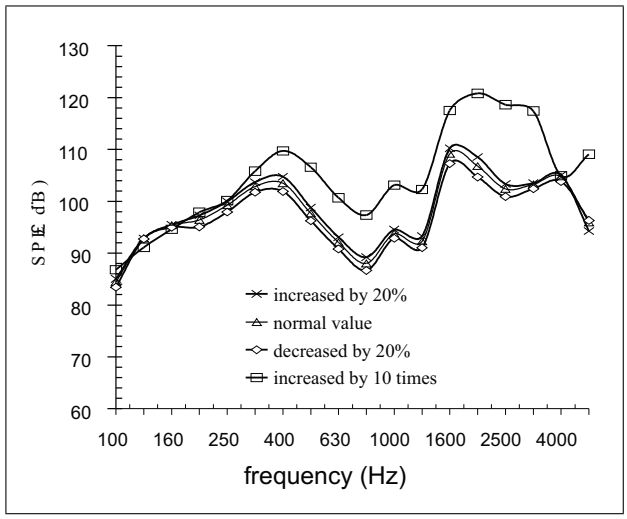

Figure 9. Influence of coating with different shear modulus μ on radiated pressure.

helpful for designing and optimizing low-noise underwater vehicles. Nevertheless, our work needs further experimental support as well as the introduction of more elaborate theoretical models for perforated viscoelastic coating.

4. Conclusions

A solution is developed for the acoustic radiation from two concentric submerged cylindrical shells with periodic supports and the outer viscoelastic perforated coating. The viscoelastic perforated coating is treated as a non-perforated one by using equivalent complex moduli. The reactive forces due to the supports and the coating are included in the loading terms of the unsupported shells. Numerical results from two infinite shells agree well with measured data taken from a finite two-walled reinforced cabin.

Further numerical results indicate that the viscoelastic perforated coating can effectively reduce the acoustic radiation, especially at high frequency ranges. Porosity ratio and shear modulus play more dominant roles in reducing the acoustic pressure than other coating parameters do. However, further mechanism of acoustic attenuation due to viscoelastic perforated coating need to be investigated systematically.

Appendix

A1. Transformed impedances

The transformed impedances of the inner shell at the n-th circumferential mode is given as [2]

$$\tilde{Z}^{s}_{1n}(k) = \frac{\mathrm{i}\rho c_l^2}{\omega a_1^2\left(\frac{1}{h_1}+\frac{1-2\gamma}{2a_1(1-\gamma)}\right)}\Big\{-\Omega_1^2+\frac{h_1^2}{24(1-\gamma)a_1^2} \cdot\Big[2(1-\gamma)(n^2+\alpha_1^2)^2-(4-\gamma)n^2+2+\gamma\Big]$$

$$+\left[\alpha_1^2(1-\gamma^2)\left[(1-\gamma)\alpha_1^2/2-\Omega_1^2\right]-\Omega_1^2\left[(1-\gamma)(\alpha_1^2+n^2)/2-\Omega_1^2\right]\right]\left[\left[(1-\gamma)(\alpha_1^2+n^2)/2-\Omega_1^2\right]\left[\alpha_1^2+n^2+\Omega_1^2\right]\right]^{-1}\Big\}, \tag{A1}$$

where ρ, γ and c_l are the mass density, poisson's ratio and longitudinal phase velocity of the two shells, respectively, $\alpha_1 = a_1 k$, $\Omega_1 = a_1\omega/c_l$. $\tilde{Z}^s_{2n}(k)$ has the same form as $\tilde{Z}^s_{1n}(k)$ once the subscripts of the symbols in equation (A1) are changed from 1 into 2.

A2. Transformed point force

The transformed point force acting on the inner shell at the n-th circumferential mode is given as follows [2],

$$\tilde{F}_n(k) = \frac{F_1}{(2\pi)^2 a_1} \mathrm{e}^{-\mathrm{i}(kx_0+n\varphi_0)}. \tag{A2}$$

Burroughs [2] treated the circular ring as a slice of cylindrical shell. He developed the transformed, reactive forces from the rings at the n-th circumferential mode as

$$\tilde{p}_{rn} = \frac{k_d}{2\pi} Z^r_n \sum_{m=-\infty}^{\infty} \dot{\tilde{w}}_{1n}(k+mk_d), \tag{A3}$$

and Z^r_n has the form

$$Z^r_n = \frac{\mathrm{i}}{\omega a_1}\frac{2\rho_r c_l'^2 A_r}{2a_1+h_r}\left[1-\overline{\Omega}_1^2+\frac{h_r^2}{12a_1^2}(n^2-1)^2+\frac{n^2}{\overline{\Omega}_1^2-n^2}\right],$$

where ρ_r, A_r and h_r are the mass density, cross-section area, thickness of the rings, c_l' is the longitudinal phase velocity of the rings and $\overline{\Omega}_1 = a_1\omega/c_l'$.

References

[1] M. C. Junger: Dynamic behavior of reinforced cylindrical shells in a vacuum and in a fluid. J. Appl. Mech. (1954) 35–41.

[2] C. B. Burroughs: Acoustic radiation from fluid-loaded infinite circular cylinders with doubly periodic supports. J. Acoust. Soc. Am. **75** (1984) 715–722.

[3] C. B. Burroughs, J. E. Hallander: Acoustic radiation from fluid-loaded, ribbed cylindrical shells excited by different types of concentrated mechanical drives. J. Acoust. Soc. Am. **91** (1992) 2721–2739.

[4] A. Klauson, J. Metsaveer: Sound scattering by a cylindrical shell reinforced by lengthwise ribs and walls. J. Acoust. Soc. Am. **91** (1992) 1834–1843.

[5] J. M. Cuschieri, D. Feit: Acoustic scattering from a fluid-loaded cylindrical shell with discontinuities: Double plate bulkhead. J. Acoust. Soc. Am. **98** (1995) 339–352.

[6] Y. P. Guo: Sound scattering by bulkheads in cylindrical shells. J. Acoust. Soc. Am. **95** (1994) 2550–2559.

[7] J. M. Cuschieri, D. Feit: A hybrid solution for the response Green's function of a fluid-loaded cylindrical shell. J. Acoust. Soc. Am. **96** (1994) 2776–2784.

[8] S. Yoshikawa, E. G. Williams, K. B. Washburn: Vibration of two concentric submerged cylindrical shells coupled by the entrained fluid. J. Acoust. Soc. Am. **95** (1994) 3273–3286.

[9] T. T. Yeh, S. S. Chen: Dynamics of a cylindrical shell system coupled by viscous fluid. J. Acoust. Soc. Am. **62** (1977) 262–270.

[10] B. Laulagnet, J. L. Guyader: Sound radiation from finite cylindrical shells, partially covered with longitudinal strips of compliant layer. J. Sound and Vibration **186** (1995) 723–742.

[11] B. Laulagnet, J. L. Guyader: Sound radiation from finite cylindrical coated shells, by means of asymptotic expansion of three-dimensional equations for coating. J. Acoust. Soc. Am. **96** (1994) 277–286.

[12] M. X. Chen, D. P. Luo, X. Peng et al.: Analysis of characteristics of sound radiation from double cylindrical shell coated with viscoelastic layer. Chinese Journal of Acoustics **23** (45-57) 2004.

[13] G. C. Gaunaurd, J. Barlow: Matrix viscosity and cavity-size distribution effects on the dynamic effective properties of perforated elastomers. J. Acoust. Soc. Am. **75** (1984) 23–34.

[14] G. C. Gaunaurd, W. Wertman: Comparison of effective medium theories for inhomogeneous continua. J. Acoust. Soc. Am. **85** (1989) 541–554.

[15] K. E. Gilbert: A propagator matrix method for periodically stratified media. J. Acoust. Soc. Am. **73** (1983) 137–142.

[16] B. H. Song, J. S. Bolton: A transfer-matrix approach for estimating the characteristic impedance and wave numbers of limp and rigid porous materials. J. Acoust. Soc. Am. **107** (2000) 1131–1152.

[17] M. C. Junger, D. Feit: Sound, structures and their interaction. MIT Press, Cambridge, MA, 1986.

[18] F. Fahy: Sound and structural vibration, radiation, transmission and response. Academic Press Inc., San Diego, 1987.

[19] X. W. Yin: Study on vibration and acoustic radiation from two concentric ring-reinforced cylindrical shells covered with sound-absorbing layers. China Ship Scientific Research Center, MSc thesis, No. S00-02-02, 2001.